OPEN ACCESS

KING'S College LONDON

King's Research Portal

DOI:
10.1148/radiol.2021201630

Link to publication record in King's Research Portal

Citation for published version (APA):
Bustin, A., Hua, A., Milotta, G., Jaubert, O., Hajhosseiny, R., Ismail, T. F., Botnar, R. M., & Prieto, C. (2021). High-Spatial-Resolution 3D Whole-Heart MRI T2 Mapping for Assessment of Myocarditis. *Radiology*, *298*(3), 578-586. https://doi.org/10.1148/radiol.2021201630

Citing this paper
Please note that where the full-text provided on King's Research Portal is the Author Accepted Manuscript or Post-Print version this may differ from the final Published version. If citing, it is advised that you check and use the publisher's definitive version for pagination, volume/issue, and date of publication details. And where the final published version is provided on the Research Portal, if citing you are again advised to check the publisher's website for any subsequent corrections.

General rights
Copyright and moral rights for the publications made accessible in the Research Portal are retained by the authors and/or other copyright owners and it is a condition of accessing publications that users recognize and abide by the legal requirements associated with these rights.

•Users may download and print one copy of any publication from the Research Portal for the purpose of private study or research.
•You may not further distribute the material or use it for any profit-making activity or commercial gain
•You may freely distribute the URL identifying the publication in the Research Portal

Take down policy
If you believe that this document breaches copyright please contact librarypure@kcl.ac.uk providing details, and we will remove access to the work immediately and investigate your claim.

Download date: 14. Jan. 2025

Radiology

ORIGINAL RESEARCH • CARDIAC IMAGING

High-Spatial-Resolution 3D Whole-Heart MRI T2 Mapping for Assessment of Myocarditis

Aurélien Bustin, PhD • Alina Hua, MD • Giorgia Milotta, MSc • Olivier Jaubert, BS • Reza Hajhosseiny, MD • Tevfik F. Ismail, MD, PhD • René M. Botnar, PhD • Claudia Prieto, PhD

From the Department of Biomedical Engineering, School of Biomedical Engineering and Imaging Sciences, King's College London, 3rd Floor, Lambeth Wing, St Thomas' Hospital, London SE1 7EH, England (A.B., A.H., G.M., O.J., R.H., T.F.I., R.M.B., C.P.); and Escuela de Ingeniería, Pontificia Universidad Católica de Chile, Santiago, Chile (R.M.B., C.P.). Received April 16, 2020; revision requested May 20; revision received September 25; accepted October 7. **Address correspondence to** C.P. (e-mail: *claudia.prieto@kcl.ac.uk*).

Supported by the Engineering and Physical Sciences Research Council (EP/P032311/1, EP/P001009/1, and EP/P007619/1), British Heart Foundation (grant no. RG/20/1/34802), King's British Heart Foundation Centre for Research Excellence (RE/18/2/34213),Wellcome Engineering and Physical Sciences Centre for Medical Engineering (NS/A000049/1), and the Department of Health through the National Institute for Health Research Cardiovascular Health Technology Cooperative and comprehensive Biomedical Research Centre awarded to Guy's and St Thomas's National Health Service Foundation Trust in partnership with King's College London and King's College Hospital National Health Service Foundation Trust.

Conflicts of interest are listed at the end of this article.

See also the editorial by Friedrich in this issue.

Radiology 2021; 00:1–9 • https://doi.org/10.1148/radiol.2021201630 • Content codes: CA MR

Background: Clinical guidelines recommend the use of established T2 mapping sequences to detect and quantify myocarditis and edema, but T2 mapping is performed in two dimensions with limited coverage and repetitive breath holds.

Purpose: To assess the reproducibility of an accelerated free-breathing three-dimensional (3D) whole-heart T2 MRI mapping sequence in phantoms and participants without a history of cardiac disease and to investigate its clinical performance in participants with suspected myocarditis.

Materials and Methods: Eight participants (three women, mean age, 31 years ± 4 [standard deviation]; cohort 1) without a history of cardiac disease and 25 participants (nine women, mean age, 45 years ± 17; cohort 2) with clinically suspected myocarditis underwent accelerated free-breathing 3D whole-heart T2 mapping with 100% respiratory scanning efficiency at 1.5 T. The participants were enrolled from November 2018 to August 2020. Three repeated scans were performed on 2 separate days in cohort 1. Segmental variations in T2 relaxation times of the left ventricular myocardium were assessed, and intrasession and intersession reproducibility were measured. In cohort 2, segmental myocardial T2 values, detection of focal inflammation, and map quality were compared with those obtained from clinical breath-hold two-dimensional (2D) T2 mapping. Statistical differences were assessed using the nonparametric Mann-Whitney and Kruskal-Wallis tests, whereas the paired Wilcoxon signed-rank test was used to assess subjective scores.

Results: Whole-heart T2 maps were acquired in a mean time of 6 minutes 53 seconds ± 1 minute 5 seconds at 1.5 mm^3 resolution. Breath-hold 2D and free-breathing 3D T2 mapping had similar intrasession (mean T2 change of 3.2% and 2.3% for 2D and 3D, respectively) and intersession (4.8% and 4.9%, respectively) reproducibility. The two T2 mapping sequences showed similar map quality (P = .23, cohort 2). Abnormal myocardial segments were identified with confidence (score 3) in 14 of 25 participants (56%) with 3D T2 mapping and only in 10 of 25 participants (40%) with 2D T2 mapping.

Conclusion: High-spatial-resolution three-dimensional (3D) whole-heart T2 mapping shows high intrasession and intersession reproducibility and helps provide T2 myocardial characterization in agreement with clinical two-dimensional reference, while enabling 3D assessment of focal disease with higher confidence.

© RSNA, 2021

Online supplemental material is available for this article.

Myocarditis is an acute or chronic inflammatory disease of the myocardium. Patients who initially recover from myocarditis can later develop complications, including dilated cardiomyopathy with significantly impaired left ventricular function, conduction system disease, arrhythmias, or sudden cardiac death (1,2). Endomyocardial biopsy remains an imperfect reference standard for assessment of myocarditis because of its low sensitivity and limited diagnostic accuracy because of sampling error and interobserver variability (3).

The widespread clinical acceptance of cardiovascular MRI for assessment of myocardial tissue characterization has rendered cardiac MRI a noninvasive diagnostic alternative in patients with suspected acute myocarditis (4,5). Comprehensive multiparametric cardiac MRI has the capability to assess global and regional cardiac function and regional myocardial blood flow and to detect focal and diffuse fibrosis and edema. Consequently, the revised 2018 Lake Louise Criteria includes multiparametric cardiovascular MRI markers, including T1 and T2 mapping, for the diagnosis of patients with suspected myocarditis (6). In particular, T2 mapping has shown good diagnostic accuracy in identifying acute myocardial edema (7,8) and can be especially useful in ruling out active myocardial inflammation.

Yet, as multiparametric cardiac MRI is more widely implemented in clinical practice, most protocols are based on established nonisotropic two-dimensional (2D) T2-weighted imaging and 2D T2 mapping protocols that

This copy is for personal use only. To order printed copies, contact *reprints@rsna.org*

Abbreviations

iNAVs = image-based navigators, LGE = late gadolinium enhancement, SSFP = steady-state free precession, STIR = short inversion time inversion recovery, 3D = three-dimensional, 2D = two-dimensional

Summary

High-resolution respiratory motion compensated accelerated three-dimensional T2 mapping enables reproducible quantification of myocardial T2 times for whole-heart assessment of myocarditis in an efficient and fast manner.

Key Results

- A free-breathing three-dimensional (3D) saturation-based T2 mapping sequence acquired T2 maps of the whole heart with 1.5 mm^3 isotropic resolution and a scanning time of less than 7 minutes.
- Compared with participants without a history of cardiac disease, myocardial T2 values were prolonged on 3D whole-heart T2 mapping in participants with suspected myocarditis (68 msec ± 7 [standard deviation] vs 51 msec ± 3).

require repetitive and long breath holds to cover the left ventricle (7,9,10). Because of the many breath holds required, often only a fraction of the left ventricle is acquired, thus potentially missing focal areas of inflammation. Moreover, the large slice thickness may also reduce the sensitivity of these sequences for edema detection because of partial volume effects.

Three-dimensional (3D) myocardial T2 mapping techniques have been proposed to provide whole-heart coverage and to potentially allow for better characterization of the complex diffuse pathologic findings, albeit with longer acquisition times (11,12). A framework for free-breathing motion-corrected 3D whole-heart T2 mapping with high isotropic resolution (1.5 mm^3) and clinically feasible scanning times (approximately 8 minutes) has recently been proposed (13). This approach showed low T2 bias in phantoms and good agreement with conventional 2D mapping in a small cohort of healthy patients, while providing 3D whole-heart coverage under free breathing with a fast and predictable scanning time.

The aim of this study was *(a)* to assess the reproducibility of this technique both in phantoms and participants without a history of cardiac disease and *(b)* to investigate its clinical performance in comparison with clinically used 2D T2 mapping and 2D T2-weighted imaging in participants with suspected myocarditis.

Materials and Methods

The prospective study was approved by the National Research Ethics Service, and written informed consent was obtained from all participants. In a previous study (13), we reported on eight healthy participants included in the current study. The previous study assessed the accuracy and spatial standard deviation (as a surrogate of precision) of 3D whole-heart T2 mapping. The current study expends on this by assessing intrasession and intersession reproducibility to further investigate the suitability of the proposed method for clinical translation.

High-Resolution 3D Whole-Heart T2 Mapping

Cardiac MRI acquisitions were performed in the supine position with a 1.5-T scanner (Magnetom Aera; Siemens Healthcare) with a 32-channel spine coil and a dedicated 18-channel body coil.

The investigated free-breathing motion-corrected 3D whole-heart T2 mapping sequence (Fig 1) was previously described in Bustin et al (13). In brief, an electrocardiogram-triggered free-breathing T2-prepared balanced steady-state free precession (SSFP) sequence is modified to include a nonselective saturation pulse after each R wave with constant saturation time to the κ-space data acquisition (11). This allows for efficient imaging at every heartbeat, thus avoiding the use of multiple R-R magnetization recovery periods and reducing the total scanning time. An adiabatic T2-prepared pulse (Silver-Hoult pair) is played before data acquisition (14), and the sequence is sequentially repeated with variable echo time of the T2 preparation (no T2 preparation, 28 msec, and 55 msec). To further accelerate the acquisition, a 5× undersampled 3D Cartesian variable-density trajectory with spiral profile order and golden angle rotation is adopted (13,15). Predictable scanning time and 100% respiratory scanning efficiency (no data rejection) are achieved using low-resolution 2D image-based navigators (iNAVs). iNAVs are acquired at every heartbeat ahead of the data acquisition by encoding the linear ramp-up pulses of the 3D balanced SSFP read-out (16) and are used to estimate and correct for superior-inferior and right-left translational respiratory motion. A template-matching algorithm with a mutual information similarity measure, robust against contrast change between images, was used to estimate the translational motion. A multi-contrast high-dimensionality undersampled patch-based reconstruction (17) jointly reconstructs the three undersampled T2-prepared volumes. The final 3D whole-heart T2 map is then generated by participant-specific (mean heart rate, trigger delay, and acquisition window) dictionary matching using the extended phase graph formalism (18).

Scan-Rescan Phantom Reproducibility Study

Scan-rescan reproducibility of the 3D T2 mapping sequence was first assessed in a phantom containing six vials with different concentrations of agarose and nickel(II) chloride and whose T1 and T2 values roughly span the relaxation times of the human myocardium before and after contrast (19).

In addition to 3D free-breathing isotropic T2 mapping (as previously described), standard three-slice 2D breath-hold T2 maps were acquired using a clinical single-shot T2-prepared balanced SSFP sequence. Details of the scanning parameters are provided in Appendix E1 (online). Additional scanning parameters for the 3D T2 mapping sequence were as follows: acquired resolution = reconstructed resolution = 1.50 × 1.50 × 1.50 mm^3; field of view, 320 × 320 × 84–132 mm^3; slice oversampling, 22%; repetition time msec/echo time msec, 3.1/1.4; flip angle, 90°; receiver bandwidth, 830 Hz per pixel; and iNAV with 14 start-up echoes.

The 2D and 3D T2 mapping sequences were repeated 10 times in a single session, with the phantom being removed and then replaced between acquisitions. A simulated heart rate of 70 beats per minute was used for cardiac triggering. Reference

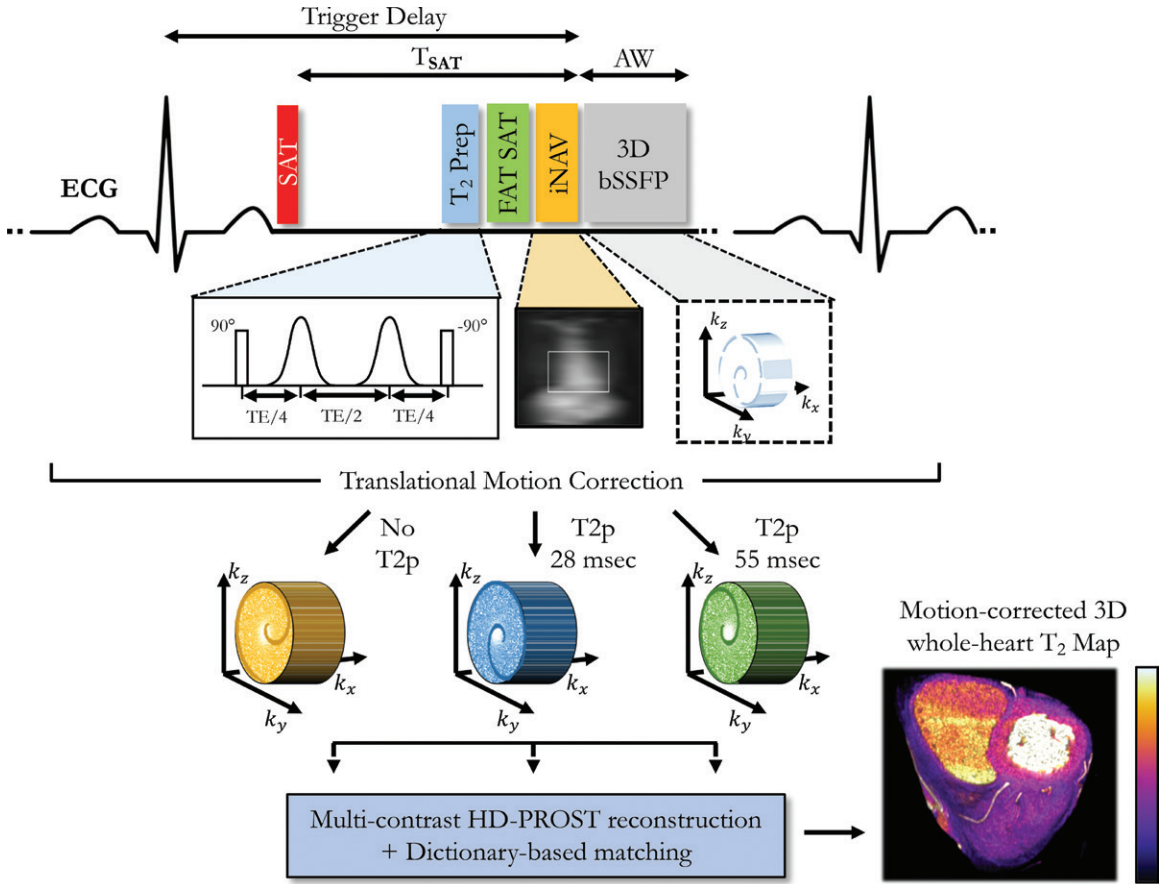

Figure 1: Schematic overview of investigated free-breathing motion-corrected three-dimensional (3D) whole-heart myocardial T2 mapping framework. Three T2-prepared (T_2 prep) volumes are acquired sequentially with increasing echo time of T2 preparation (no T2 preparation, 28 msec, and 55 msec). A nonselective saturation pulse (SAT) is applied immediately after electrocardiogram (ECG) R wave to avoid magnetization recovery heartbeats. A two-dimensional image navigator is acquired to enable translational respiratory motion correction of heart and shorter and predictable scanning times. A golden-angle shifted variable-density Cartesian undersampling is used to achieve clinically feasible scanning times. The three T2-prepared volumes are jointly reconstructed with a high-dimensionality undersampled patch-based reconstruction (HD-PROST). A dictionary, based on extended phase graph algorithm, is then simulated and matched to measured signal to generate 3D whole-heart T2 map. AW = acquisition window, bSSFP = balanced steady-state free precession, FAT = fat suppression, iNAV = image-based navigator, k_x = readout, k_y = phase encoding, k_z = slice selection, TE = echo time, T_{SAT} = saturation time.

T2 values were established using a conventional spin-echo sequence.

Intrasession and Intersession in Vivo Reproducibility Study

Eight adult participants (cohort 1; three women; mean age, 31 years ± 4 [standard deviation]; range, 26–36 years; body mass index, 22.6 kg/m^2 ± 3.1) with no history of heart disease or known cardiovascular risk factors were enrolled in the study. To assess intrasession and intersession reproducibility, each participant underwent three cardiac MRI examinations on 2 distinct days. The median interval between the two sessions was 347 days (range, 343–354 days). In the first session, the breath-hold 2D and investigated free-breathing 3D T2 mapping sequences were performed in random order. In the second session, the 2D and 3D sequences were randomly performed twice with the participant being removed from the bed and then repositioned. The 2D and 3D T2 mapping sequences were performed with the same parameters prescribed in the phantom study. Additional scanning parameters for the 3D T2 mapping sequence are provided in Appendix E1 (online).

Evaluation in Participants with Clinically Suspected Myocarditis

Twenty-five adult participants (cohort 2; nine women; mean age, 45 years ± 17; range, 19–76 years; body mass index, 25.1 kg/m^2 ± 4.9) with suspected myocarditis and presenting with chest pain, raised troponin, and unobstructed coronary arteries were prospectively recruited for a clinical cardiac MRI at St Thomas between November 2018 and August 2020. Characteristics of cohorts 1 and 2 are presented in Table 1. The cardiac MRI protocol consisted of a conventional clinical myocarditis protocol with additional free-breathing 3D whole-heart myocardial T2 mapping (Appendix E1 and Table E1 [online]).

Statistical Analysis

A detailed description of phantom and cardiac MRI data analysis is provided in Appendix E1 (online). In participants, all T2 map data sets (clinical 2D and proposed 3D whole heart) were anonymized and randomly stored for qualitative assessment by an experienced cardiologist (T.F.I., with 10 years of experience and Society for Cardiovascular Magnetic Resonance level III certification). Map quality was assessed using a four-point scoring system with

Table 1: Characteristics of Cohorts 1 and 2

Characteristic	Cohort 1 (Volunteers)	Cohort 2 (Participants)
No. of participants	8	25
Sex (F/M)	3/5	9/16
Age (y)*	31 ± 4 (26–36)	45 ± 17 (19–76)
Heart rate (beats/min)*	65 ± 10 (54–82)	61 ± 10 (47–81)
Body mass index (kg/m^2)†	23 ± 3	25 ± 5
Impaired left ventricular function	…	4 (16)
Presence of LGE	…	11 (44)
Pattern of LGE	…	
Midwall LGE	…	8 (73)
Subendocardial LGE	…	3 (27)
Pericarditis	…	5 (20)
Myocarditis	…	11 (44)
Elevated T2-weighted SI ratio	…	8 (32)

Note.—Except where indicated, data are numbers of participants, with percentages in parentheses. LGE = late gadolinium enhancement, SI = signal intensity.

* Numbers are means ± standard deviations, with ranges in parentheses.

† Numbers are means ± standard deviations.

1 indicating nondiagnostic (poor image quality with complete distortion), 2 indicating acceptable and/or fair image quality (partial distortion on the T2 map but diagnosis can be made in some segments), 3 indicating good (no distortion on the T2 map but spatial blurring), and 4 indicating excellent (full-diagnostic, sharp T2 map). Diagnostic confidence was rated with a three-point scale (1 indicating low confidence, and 3 indicating high confidence).

Statistical analysis was performed with IBM SPSS Statistics software (version 26.0). Continuous variables were presented as mean ± standard deviation. The Kolmogorov-Smirnov test was used to test the null hypothesis that each continuous variable follows a normal distribution. The Mann-Whitney *U* test was used to compare differences in continuous variables between two groups if the distribution was not normal. The Student *t* test was used for normal distribution. For the comparison of three or more independent groups, a one-way analysis of variance was used for normal distributions, whereas the Kruskal-Wallis rank test was used for nonnormal distributions. T2 differences between slices and segments were evaluated by repeated-measures analysis of variance and Bonferroni correction. Subjective scores were compared with a paired Wilcoxon signed-rank test to assess statistical differences. Two-tailed values of $P < .05$ were considered statistically significant differences. T2 bias in the phantom was quantified with Bland-Altman analysis.

Results

Scan-Rescan Phantom Reproducibility

Phantom results are summarized in Table 2 for each of the six vials. On average, interscan variation was lower with 3D T2 mapping compared with conventional 2D T2-prepared balanced SSFP (0.1 msec vs 0.2 msec ± 0.1, $P < .01$). Similarly, T2 bias (1.3 msec ± 0.9 vs 4.9 msec ± 3.6, $P = .04$) and signed bias (0.2 msec ± 1.7 vs −4.9 msec ± 3.6, $P = .01$) with respect to reference spin-echo T2 mapping were lower with the investigated 3D technique. Overall, T2 spatial variability (ie, mean of standard deviations) was found to be higher with the 3D technique (2.5 msec ± 0.9 vs 1.1 msec ± 0.3, $P < .01$).

Description of the Study Participants

All in vivo scans were successful and suitable for analysis. Characteristics of the study participants are summarized in Table 1 and study flow diagram outlining the selection and analysis of participants is shown in Figure 2. Myocarditis involvement was the predominant clinical finding in 11 of 25 participants (44%) in cohort 2. Eleven participants (44%) had presence of late gadolinium enhancement (LGE) with a predominant midwall pattern in eight of them (73%). Five participants (20%) presented with pericarditis. Eight participants (32%) also had evidence of increased T2 signal intensity at T2-weighted short inversion time inversion recovery (STIR) imaging.

Intrasession and Intersession in Vivo Reproducibility in Healthy Participants

Eight study participants were evaluated for reproducibility. The average acquisition time of the investigated free-breathing 3D whole-heart T2 mapping sequence in cohort 1 participants was 6 minutes 29 seconds ± 1 minute 8 seconds (scan 1, session 1), 6 minutes 8 seconds ± 50 seconds (scan 2, session 2), and 6 minutes 11 seconds ± 42 seconds (scan 3, session 2) with 100% respiratory scanning efficiency and predictable scanning times. There were no statistical differences between scanning times ($P = .66$).

T2 values obtained for each myocardial segment (according to the American Heart Association 16-segment model) for the 2D (breath-hold) and 3D (free-breathing) T2 mapping sequences are presented in Figure E1 (online) for the first session only. There were no statistical differences between segments on a basal ($P = .68$), midcavity ($P = .77$), and apical ($P = .53$) level for the 3D T2 mapping sequence. Similar results were observed for the 2D T2 mapping sequence.

Averaged T2 values (among the eight participants) were significantly different between 2D and 3D T2 mapping for the first scan for the basal slices (2D, 44 msec ± 1; 3D, 50 msec ± 2; $P < .01$) but were not found statistically different for the midcavity (2D, 47 msec ± 4; 3D, 49 msec ± 2; $P = .08$) and apical (2D, 49 msec ± 4; 3D, 49 msec ± 3; $P = .65$) slices (Fig 3). T2 values for scans 2 and 3 are presented in Figure E2 (online) and agreed with those findings.

The intersession reproducibility, as represented by the septal T2 difference between scans 1 and 3, is shown in Figure 3. There was a statistically significant difference between 2D and 3D T2 mapping for the midcavity slices ($P = .03$), whereas 2D and 3D T2 mapping had similar intersession reproducibility for the basal ($P = .96$) and apical ($P = .80$) slices. Breath-hold 2D and free-breathing 3D T2 mapping had similar intrasession reproducibility for all slices (basal, $P = .44$; midcavity, $P = .51$; apical, $P = .96$). The intersession mean T2 change was 4.8% and 4.9% for 2D and 3D T2

Table 2: Reproducibility Phantom Results for 2D and 3D T2 Mapping

	T1/T2 References		T2 Spatial Variability (msec)		T2 Interscan Variation (msec)		T2 Accuracy (msec)		T2 Signed Accuracy Bias (msec)	
Vial No.	Spin-echo T1 (msec)	Spin-echo T2 (msec)	3D T2 Mapping	2D T2 Mapping	3D T2 Mapping	2D T2 Mapping	3D T2 Mapping	2D T2 Mapping	3D T2 Mapping	2D T2 Mapping
1	430	44	3.3	0.8	0.1	0.3	0.1	5.0	0.1	−5.0
2	458	45	3.9	1.2	0.1	0.1	0.4	3.4	−0.4	−3.4
3	1090	48	1.8	1.2	0.1	0.3	2.3	6.5	2.3	−6.5
4	803	48	2.0	0.9	0.1	0.3	2.1	2.6	2.1	−2.6
5	300	44	2.4	1.8	0.1	0.2	1.2	11.1	−1.2	−11.1
6	1333	50	1.4	1.0	0.1	0.2	1.8	0.8	−1.8	−0.8
Average*	…	…	2.5 ± 0.9	1.1 ± 0.3	0.1	0.2 ± 0.1	1.3 ± 0.9	4.9 ± 3.6	0.2 ± 1.8	−4.9 ± 3.6

Note.—Spatial variability was measured in each vial as the average (over 10 repetitions) of the standard deviation of T2 measurements obtained with each sequence. Interscan variation was measured in each vial as the standard deviation of T2 measurements over 10 repetitions. Bias in T2 was measured in each vial as the average (over 10 repetitions) of the absolute difference between T2 measurements obtained from reference spin-echo and each sequence. T2 signed bias was measured in each vial as the difference between spin-echo T2 measurements and the average (over 10 repetitions) of the T2 measurements obtained with each sequence. *P* values for three-dimensional (3D) versus two-dimensional (2D) mapping were less than .01 for T2 spatial variability and T2 interscan variation, .04 for T2 accuracy, and .01 for T2 signed accuracy bias.

* Numbers are means ± standard deviations.

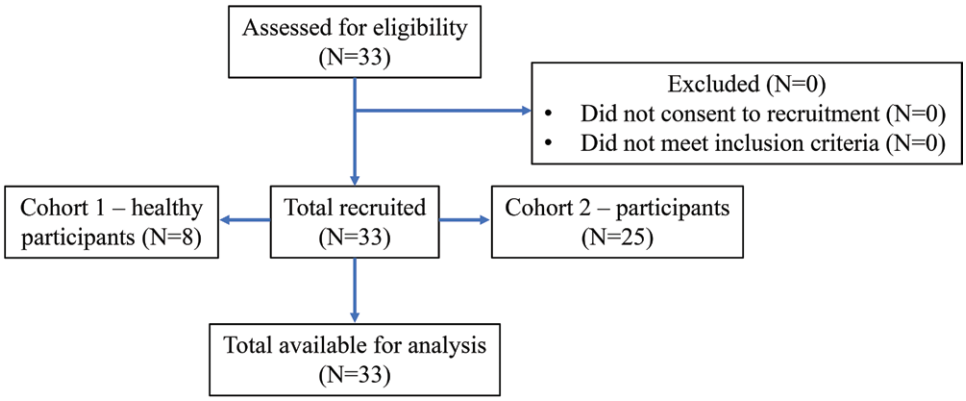

Figure 2: Study flowchart outlines the selection and analysis of healthy participants (cohort 1, *n* = 8) and participants with suspected myocarditis (cohort 2, *n* = 25).

mapping, respectively, whereas the intrasession mean T2 change was 3.2% and 2.3% for 2D and 3D T2 mapping, respectively.

Evaluation in Patients with Suspected Myocarditis

The average acquisition time of the free-breathing 3D T2 mapping sequence in cohort 2 was 6 minutes 53 seconds ± 1 minute 5 seconds with 100% respiratory scanning efficiency (range, 4 minutes 41 seconds to 9 minutes 56 seconds). The mean heart rate was 61 ± 10 beats per minute, ranging from 47 to 81 beats per minute. Four of 25 participants (16%) had reduced left ventricular ejection fraction (<50%). Eleven of 25 participants (44%) had positive findings on LGE images.

In 11 of 25 participants (44%), cardiac findings were absent with confidence (score 3) in both the 2D T2 mapping and the 3D T2 mapping images, and in 10 of 25 participants (40%), there was agreement about the presence of myocardial inflammation between the two techniques. In four (16%) further participants, the presence of cardiac inflammation was found with confidence (score 3) in 3D T2 mapping; however, interpretation of the corresponding 2D T2 mapping images was inconclusive (score 1).

Free-breathing 3D T2 mapping showed significantly higher remote T2 values than breath-hold 2D T2 mapping on basal (50 msec ± 3 vs 48 msec ± 3, $P <$ .01), midcavity (50 msec ± 3 vs 47 msec ± 3, $P <$ .01), and apical (50 msec ± 3 vs 48 msec ± 3, $P =$ .02) slices (Fig E3 [online]). There were no statistically significant differences in mean remote T2 values between slices for 2D ($P =$ .68) and 3D ($P =$ .90) T2 mapping.

Short-axis 2D and 3D T2 maps with corresponding T2-weighted STIR and LGE are shown in Figure 4 for a representative participant who demonstrated normal findings at cardiac MRI. No noticeable residual undersampling artifacts were observed on the 3D T2 maps.

Among the 25 participants in cohort 2, 14 (56%) had abnormal myocardial segments as identified on the 3D T2 maps. Compared with remote segments and cohort 1 participants, average T2 values in injured segments were elevated on both 2D (65 msec ± 10) and 3D (68 msec ± 7) T2 mapping, also in agreement with an increase in signal intensity on T2-weighted STIR images (1.6 ± 0.3 vs 2.5 ± 0.8, $P <$ .05).

Image quality was considered good or excellent (graded categories 3 and 4) in 22 of 25 participants (88%) for the clinical 2D T2 mapping and in 21 of 25 participants (84%) for the 3D whole-heart T2 mapping. A grade of 2 (satisfactory) was given to the remaining three participants (12%) for 2D mapping and four participants (16%) for 3D whole-heart T2 mapping. There was no statistical difference in terms of image quality between the two sequences ($P =$ .69).

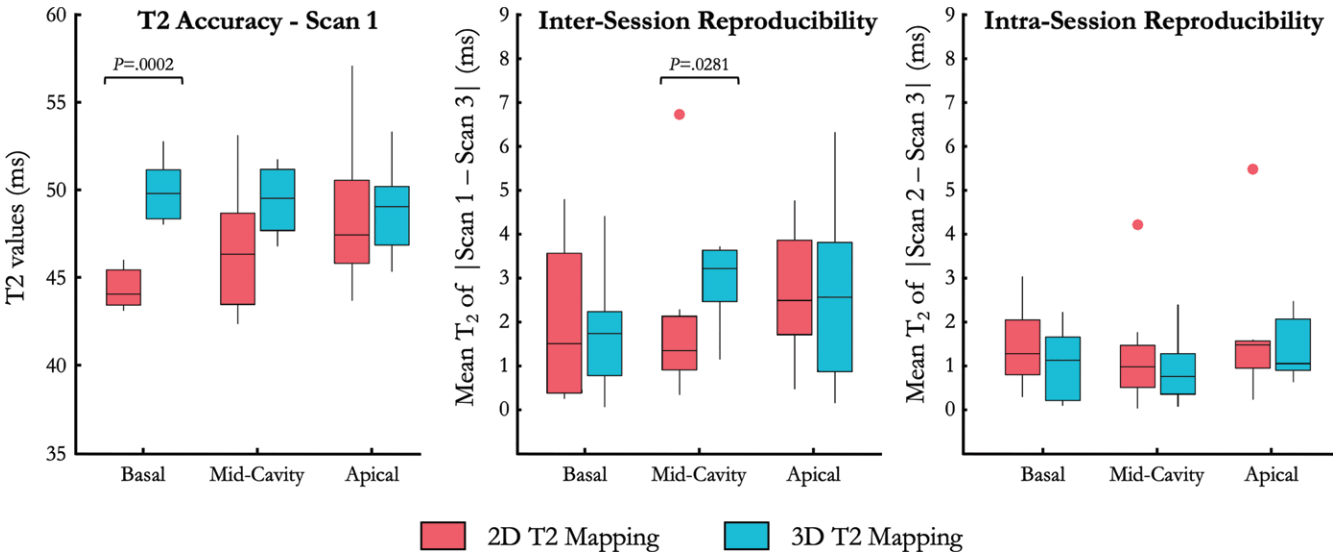

Figure 3: Box-and-whisker plots show measured T2 values and intersession and intrasession reproducibility of the investigated three-dimensional (3D) whole-heart T2 mapping framework in comparison with conventional two-dimensional (2D) T2 mapping in cohort 1 participants (no history of cardiac disease). Median is shown as line in center of box, with vertical lines indicating range from minimum to maximum value. Outliers are plotted as individual dots.

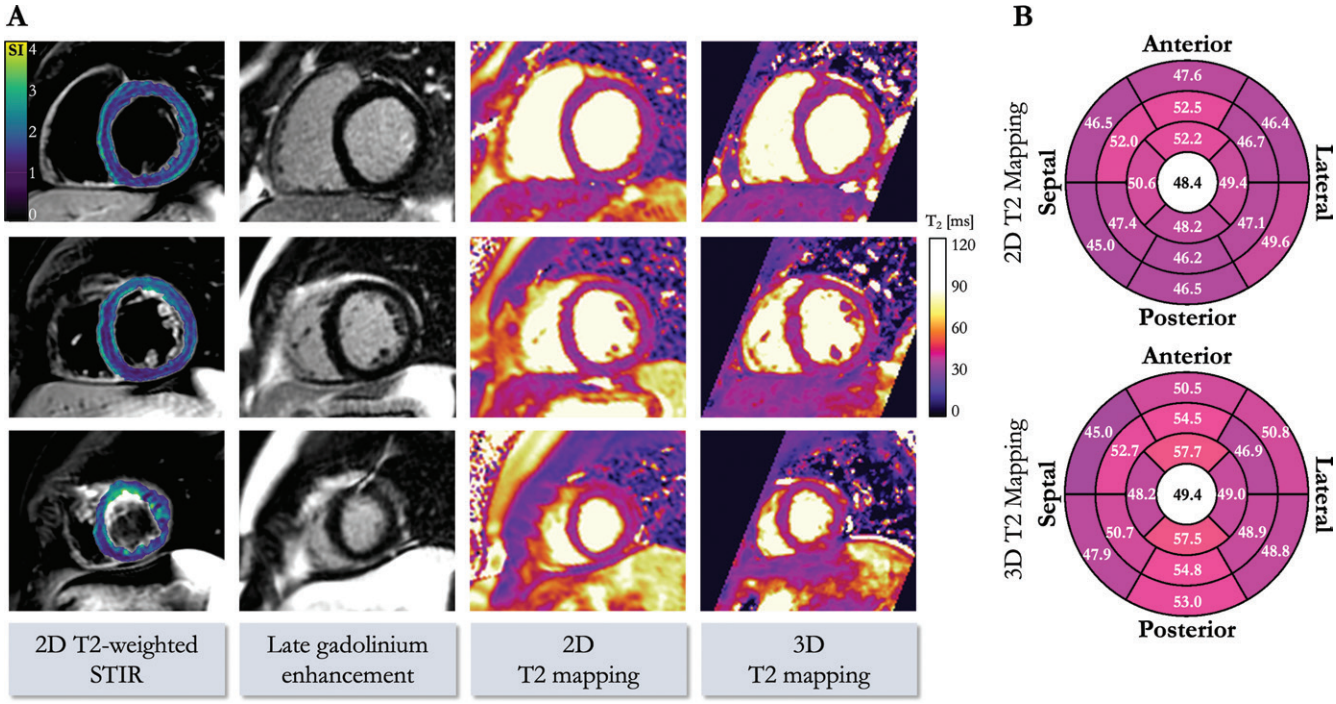

Figure 4: *A*, Cardiac MRI scans in 29-year-old female participant (cohort 2) with history of systemic lupus erythematosus demonstrate normal findings with no late gadolinium enhancement. Note signal enhancement on T2-weighted short inversion time inversion recovery (STIR) images on anterior wall at apical level, most likely because of slow blood flow. *B*, Two-dimensional (2D) (48 msec) and three-dimensional (3D) (49 msec) T2 maps show normal mean T2 values (msec) across left ventricle. Acquisition time for 3D T2 mapping was 7 minutes 5 seconds with 100% respiratory scanning efficiency. SI = signal intensity.

The entire extent of inflammation can be visualized on the 3D T2 map, which also closely matches the 2D T2 map, as shown in Figure 5, *A,* for a 61-year-old woman presenting with transmurally increased myocardial signal intensity at 2D T2-weighted STIR imaging in the midanterolateral wall, also detectable on the bull's eye plot (Fig 5, *B*).

Images in a 41-year-old man with suspected cardiac sarcoidosis are shown in Figure 6. Regions of increased T2 values on the 3D T2 map (T2, 65 msec) were in good agreement with the areas of signal enhancement observed on LGE images, T2-weighted STIR images (signal intensity, 2.1 arbitrary units), and reference 2D T2 map (T2, 61 msec). Three focal areas of increased T2 values can also be appreciated with 3D T2 mapping on the reformatted vertical long-axis view, which is in good agreement with LGE findings (Fig 6, *A*).

Another 52-year-old man with suspected cardiac involvement and reduced left ventricular ejection fraction at cardiac cine MRI (left ventricular ejection fraction, 47%) is shown in Figure E4

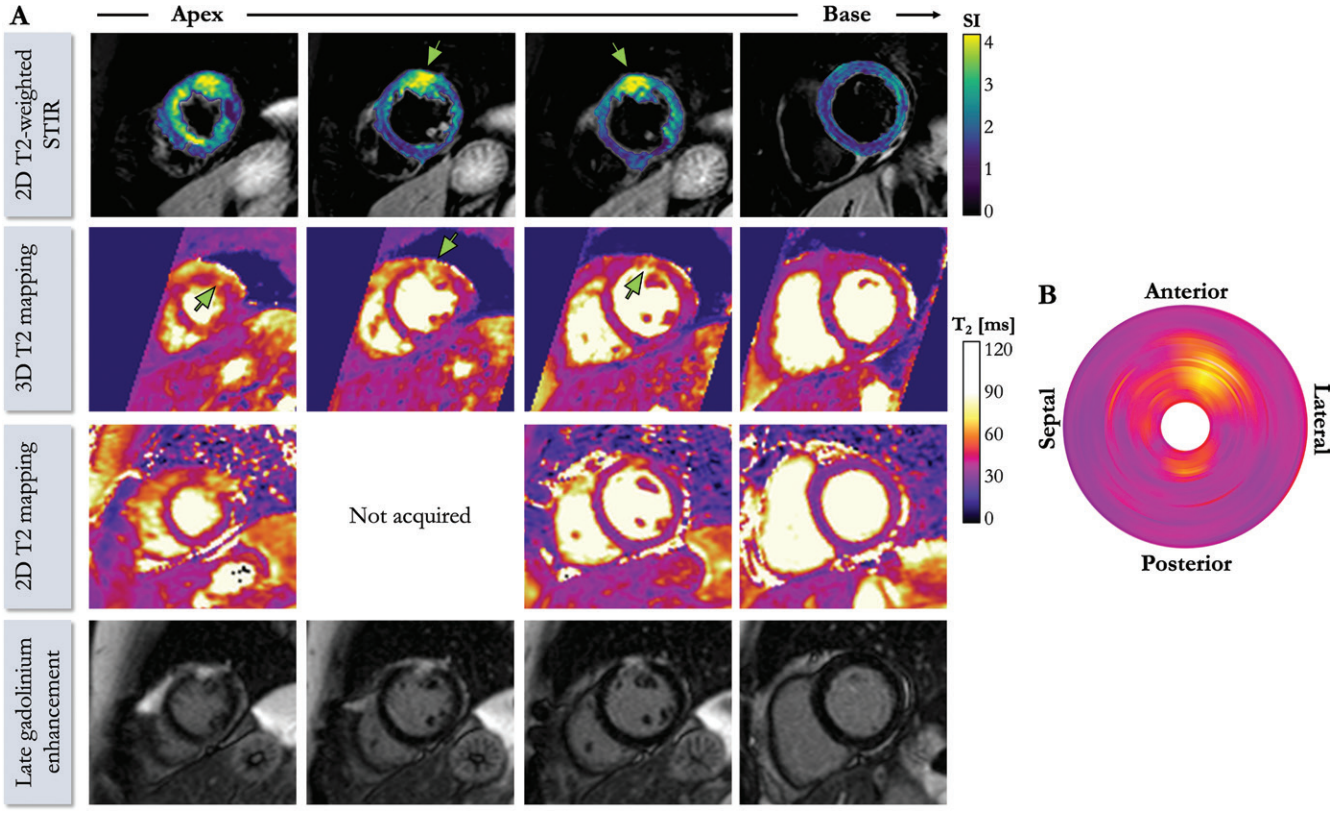

Figure 5: *A*, Cardiac MRI scans in 61-year-old female participant (cohort 2) with embolic myocardial infarction admitted to hospital with chest pain and minor coronary disease at x-ray angiography show focal transmural increased myocardial signal intensity (SI) in midanterolateral wall on T2-weighted short inversion time inversion recovery (STIR) images. Further distinct area of focal transmural enhancement is seen in apex. Subendocardial late gadolinium enhancement can be observed in midanterior and/or anterolateral wall, which toward apex becomes near transmural. 2D = two-dimensional, 3D = three-dimensional. *B*, Half of tissue injury was not detected with conventional three-slice 2D T2 mapping, whereas 3D T2 map reveals larger extent of myocardial injury (arrows), as shown on this bull's eye plot. Acquisition of 3D whole-heart T2 map took 5 minutes 29 seconds.

(online). LGE and T2-weighted STIR imaging reveal increased signal intensity in the basal to midlateral wall of the left ventricle (signal intensity, 4.3), which was confirmed by an increase of T2 values in the same region (2D, T2, 76 msec; 3D, T2, 76 msec).

Discussion

In this study, we have shown that in phantom and healthy participants, free-breathing high-resolution isotropic three-dimensional whole-heart myocardial T2 mapping enables reproducible quantification of myocardial T2 times (intersession and intrasession mean T2 change of less than 5%) in an efficient (no data rejection) and fast manner. In paarticipants with myocarditis, this framework enables whole-heart detection of cardiac involvement in a scanning time of 6 minutes 53 seconds ± 1 minute 5 seconds with 100% efficiency by virtue of the use of an image-guided navigator.

Quantitative myocardial T2 mapping is a powerful and promising tool for edema characterization and detection of subtle myocardial tissues changes in a variety of heart diseases (7,20–22). In many of these pathologic findings, the diseased area can have complex lesion morphologic characteristics, yet clinical protocol recommends the use of 2D multislice sequences, requiring several breath holds to acquire three to five short-axis slices of the heart. Such sequences are generally sufficient for patients with diffuse inflammation. However, for some cardiac diseases such as cardiac sarcoidosis, where focal patchy infiltrations of the cardiac muscle are typical pathologic manifestations, multislice sequences with limited coverage are likely to miss focal and small areas of inflammation. Two-dimensional sequences also use relatively thick slices (typically 8–10 mm) with the result that actual T2 times may be underestimated because of partial volume averaging effects, thereby potentially lowering sensitivity or resulting in an underestimation of the extent of tissue injury.

Free-breathing diaphragmatic navigated (11) and self-navigated (12) myocardial T2 mapping techniques have been proposed to achieve significantly higher spatial resolution and 3D whole-heart coverage. A saturation-based 3D myocardial T2 mapping technique (11) with diaphragmatic navigation (30%–60% scanning efficiency) has been proposed by Ding et al (23) and employed and validated for edema detection in a swine model of myocardial infarction. Van Heeswijk et al (12) proposed a self-navigated T2-prepared balanced SSFP T2 mapping sequence with 100% respiratory scanning efficiency and 1.72 mm^3 isotropic resolution at 3 T that was successfully employed for the detection of mild acute cellular rejection after orthotopic heart transplant (24); however, the scanning time was approximately 18 minutes. Notwithstanding these promising clinical results, quantification of myocardial T2 values with high isotropic resolution comes with the caveat of rather long or unpredictable scanning times. The framework evaluated in this study achieves free-breathing motion-corrected

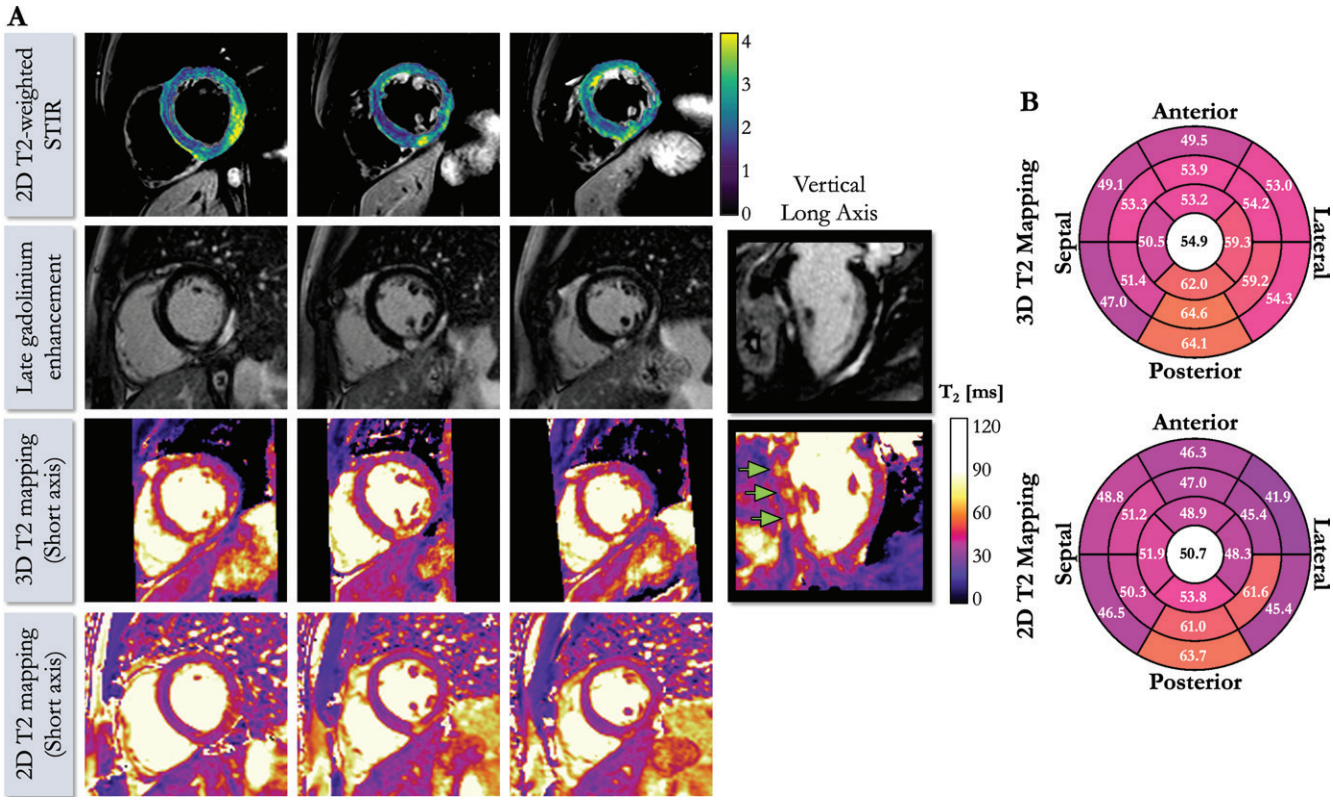

Figure 6: *A*, Cardiac MRI scans in 41-year-old male participant (cohort 2) with suspected cardiac sarcoidosis. Free-breathing three-dimensional (3D) whole-heart T2 mapping acquisition time was 7 minutes 8 seconds. Cardiac cine acquisitions reveal slightly reduced left ventricular ejection fraction (46%). Dense epicardial-to-midwall enhancement of basal to midinferior and lateral walls can be observed, which are typical findings of acute myocarditis. Vertical long axis demonstrates patchy focal midwall regions of enhancement (arrows). *B*, Three-dimensional and two-dimensional (2D) T2 maps. Three-dimensional map shows an increase in T2 values (msec) in regions of tissue injury, corresponding to elevation in signal intensity on 2D T2-weighted STIR images (signal intensity, 2.1). This T2 elevation is less pronounced and appreciable on 2D T2 maps because of partial volume effects. STIR = short inversion time inversion recovery.

3D whole-heart T2 mapping with high isotropic resolution (1.5 mm^3) and clinically feasible scanning times (approximately 7 minutes) (13). This approach provides predictable and shorter scanning times that depend only on the participant's heart rate and the number of slices needed to cover the heart.

The scan-rescan reproducibility of this 3D T2 mapping sequence (11) was analyzed in phantom experiments in comparison to reference spin-echo and clinical single-shot 2D T2-prepared balanced SSFP sequences. Small bias is obtained with the investigated sequence compared with reference spin-echo values with low T2 interscan variation (< 0.01 msec), indicating the ability of the framework to accurately measure T2 relaxation times. A slightly higher spatial variability was observed in a phantom with the proposed 3D sequence compared with the conventional 2D T2 mapping sequence (2.5 ± 0.9 vs 1.10 ± 3, $P < .01$). This could be explained by the increased resolution and the use of saturation pulses at every heartbeat, which make the sequence more sensitive to noise.

The measurements of myocardial T2 values with the free-breathing 3D whole-heart T2 mapping sequence in participants without a history of cardiac disease were in good agreement with in vivo values published in previous studies at 1.5 T with centric ordering (T2, 50 msec $\pm$ 4 [25]). Intersession reproducibility was also good in these participants with similar reproducibility between breath-hold 2D T2 mapping and free-breathing 3D T2 mapping for all basal, midcavity, and apical slices ($P > .05$).

A slight overestimation of T2 values was observed with respect to the conventional breath-hold 2D T2-prepared balanced SSFP sequence, particularly at the basal level. This overestimation may be due to the choice of linear (2D T2-prepared balanced SSFP) versus centric (3D T2 mapping) κ-space ordering as previously reported by Giri et al (7). Other confounding factors, such as the use of fat saturation and adiabatic T2-prepared pulses, motion correction, or the presence of heart-rate variations, could also explain the overestimation in vivo and should be further investigated. The precision and accuracy of the estimated T2 relaxation times also depend on the selection and duration of the T2 preparations. The selection of these parameters can be optimized using the Cramér-Rao Lower Bound formalism (26) and is currently under investigation.

The remote septal T2 values measured in the 25 participants with suspected myocarditis were comparable to those of the healthy participants. Clinical evaluation of 3D whole-heart T2 mapping in participants revealed the potential of this technique in imaging myocarditis and identifying focal areas of increased T2 values in agreement with LGE findings. Good agreement between the conventional 2D T2 mapping sequence and the investigated 3D whole-heart T2 mapping sequence was observed in 10 participants (40%) with presence of cardiac involvement. In four additional participants (16%), 3D T2 mapping showed myocardial inflammation with confidence, whereas findings from conventional 2D T2 mapping were inconclusive. In those participants with

cardiac involvement, an elevation in T2 values was found on 3D T2 mapping (68 msec ± 7) with an increase in signal intensity on the corresponding T2-weighted STIR images. Although further analysis in a larger cohort is needed, this visual assessment provides an initial indication that myocardial 3D T2 mapping may be a viable tool for the visualization of inflammation and may potentially afford improved sensitivity.

Acquisition of T2 maps with high isotropic resolution facilitates retrospective multiplanar reformatting of standard cardiac views without loss of resolution as shown in Figure 6 for a participant with patchy enhancement. The presence of small areas of inflammation can thus be assessed without acquiring additional angulated slabs, as it is often required with conventional 2D T2-weighted STIR and T2 mapping imaging.

This study had several limitations. Although two-dimensional (2D) image-based navigators (iNAVs) drastically reduce the scanning time by achieving 100% scanning efficiency, this technique only enables 2D translational respiratory motion correction of the heart. For improved performance, 2D iNAVs can be combined with a three-dimensional (3D) nonrigid motion-compensated framework, similar to previous studies (27,28); this could be used to estimate and integrate 3D nonrigid motion fields between different respiratory states directly in the reconstruction. Furthermore, echocardiographic triggering was performed in this study to restrict the acquisition to middiastole, where the heart is relatively still. Triggering can be challenging in patients with arrhythmia, where the diastolic onset and R-R intervals are erratic. Although this behavior was not observed in our study, the integration of arrythmia detection and rejection algorithms could help prevent residual cardiac motion artifacts in such populations (at the cost of losing data and thus scanning efficiency). Moreover, because T2 values have been shown to correlate with age and sex (29), the difference in age between the study participants may account for discrepancy between the two cohorts. The small sample size was also a limitation. Future studies including larger cohorts with myocarditis and myocardial infarction are needed to further establish the clinical use and prognostic value of this noninvasive mapping technique.

Author contributions: Guarantors of integrity of entire study, A.B., C.P.; study concepts/study design or data acquisition or data analysis/interpretation, all authors; manuscript drafting or manuscript revision for important intellectual content, all authors; approval of final version of submitted manuscript, all authors; agrees to ensure any questions related to the work are appropriately resolved, all authors; literature research, A.B., A.H., O.J., T.F.I., C.P.; clinical studies, A.B., G.M., R.H., T.F.I.; experimental studies, A.B., G.M., O.J., C.P.; statistical analysis, A.B., T.F.I.; and manuscript editing, A.B., A.H., G.M., R.H., T.F.I., R.M.B., C.P.

Disclosures of Conflicts of Interest: **A.B.** disclosed no relevant relationships. **A.H.** disclosed no relevant relationships. **G.M.** disclosed no relevant relationships. **O.J.** disclosed no relevant relationships. **R.H.** disclosed no relevant relationships. **T.F.I.** disclosed no relevant relationships. **R.M.B.** disclosed no relevant relationships. **C.P.** disclosed no relevant relationships.

References

1. Sagar S, Liu PP, Cooper LT Jr. Myocarditis. Lancet 2012;379(9817):738–747.
2. Maron BJ, Towbin JA, Thiene G, et al. Contemporary definitions and classification of the cardiomyopathies: an American Heart Association Scientific Statement from the Council on Clinical Cardiology, Heart Failure and Transplantation Committee; Quality of Care and Outcomes Research and Functional Genomics and Translational Biology Interdisciplinary Working Groups; and Council on Epidemiology and Prevention. Circulation 2006;113(14):1807–1816.
3. Cunningham KS, Veinot JP, Butany J. An approach to endomyocardial biopsy interpretation. J Clin Pathol 2006;59(2):121–129.
4. Abdel-Aty H, Boyé P, Zagrosek A, et al. Diagnostic performance of cardiovascular magnetic resonance in patients with suspected acute myocarditis: comparison of different approaches. J Am Coll Cardiol 2005;45(11):1815–1822.
5. Sanguineti F, Garot P, Mana M, et al. Cardiovascular magnetic resonance predictors of clinical outcome in patients with suspected acute myocarditis. J Cardiovasc Magn Reson 2015;17(1):78.
6. Ferreira VM, Schulz-Menger J, Holmvang G, et al. Cardiovascular Magnetic Resonance in Nonischemic Myocardial Inflammation: Expert Recommendations. J Am Coll Cardiol 2018;72(24):3158–3176.
7. Giri S, Chung YC, Merchant A, et al. T2 quantification for improved detection of myocardial edema. J Cardiovasc Magn Reson 2009;11(1):56.
8. Park CH, Choi EY, Kwon HM, et al. Quantitative T2 mapping for detecting myocardial edema after reperfusion of myocardial infarction: validation and comparison with T2-weighted images. Int J Cardiovasc Imaging 2013;29(S1,Suppl 1):65–72.
9. Fernández-Jiménez R, Sánchez-González J, Aguero J, et al. Fast T2 gradient-spin-echo (T2-GraSE) mapping for myocardial edema quantification: first in vivo validation in a porcine model of ischemia/reperfusion. J Cardiovasc Magn Reson 2015;17(1):92.
10. Sprinkart AM, Luetkens JA, Träber F, et al. Gradient Spin Echo (GraSE) imaging for fast myocardial T2 mapping. J Cardiovasc Magn Reson 2015;17(1):12.
11. Ding H, Fernandez-de-Manuel L, Schär M, et al. Three-dimensional whole-heart T2 mapping at 3T. Magn Reson Med 2015;74(3):803–816.
12. van Heeswijk RB, Piccini D, Feliciano H, Hullin R, Schwitter J, Stuber M. Self-navigated isotropic three-dimensional cardiac T2 mapping. Magn Reson Med 2015;73(4):1549–1554.
13. Bustin A, Milotta G, Ismail TF, Neji R, Botnar RM, Prieto C. Accelerated free-breathing whole-heart 3D T_2 mapping with high isotropic resolution. Magn Reson Med 2020;83(3):988–1002.
14. Nezafat R, Stuber M, Ouwerkerk R, Gharib AM, Desai MY, Pettigrew RI. B1-insensitive T2 preparation for improved coronary magnetic resonance angiography at 3 T. Magn Reson Med 2006;55(4):858–864.
15. Prieto C, Doneva M, Usman M, et al. Highly efficient respiratory motion compensated free-breathing coronary MRA using golden-step Cartesian acquisition. J Magn Reson Imaging 2015;41(3):738–746.
16. Henningsson M, Koken P, Stehning C, Razavi R, Prieto C, Botnar RM. Whole-heart coronary MR angiography with 2D self-navigated image reconstruction. Magn Reson Med 2012;67(2):437–445.
17. Bustin A, Lima da Cruz G, Jaubert O, Lopez K, Botnar RM, Prieto C. High-dimensionality undersampled patch-based reconstruction (HD-PROST) for accelerated multi-contrast MRI. Magn Reson Med 2019;81(6):3705–3719.
18. Weigel M. Extended phase graphs: dephasing, RF pulses, and echoes - pure and simple. J Magn Reson Imaging 2015;41(2):266–295.
19. Captur G, Gatehouse P, Keenan KE, et al. A medical device-grade T1 and ECV phantom for global T1 mapping quality assurance-the T_1 Mapping and ECV Standardization in cardiovascular magnetic resonance (T1MES) program. J Cardiovasc Magn Reson 2016;18(1):58.
20. Haberkorn SM, Spieker M, Jacoby C, Flögel U, Kelm M, Bönner F. State of the Art in Cardiovascular T2 Mapping: on the Way to a Cardiac Biomarker? Curr Cardiovasc Imaging Rep 2018;11(7):15.
21. He T, Gatehouse PD, Anderson LJ, et al. Development of a novel optimized breath-hold technique for myocardial T2 measurement in thalassemia. J Magn Reson Imaging 2006;24(3):580–585.
22. Guo H, Au WY, Cheung JS, et al. Myocardial T2 quantitation in patients with iron overload at 3 Tesla. J Magn Reson Imaging 2009;30(2):394–400.
23. Ding H, Schar M, Zviman MM, Halperin HR, Beinart R, Herzka DA. High-resolution quantitative 3D T2 mapping allows quantification of changes in edema after myocardial infarction. J Cardiovasc Magn Reson 2013;15(Supplement 1):P181.
24. van Heeswijk RB, Piccini D, Tozzi P, et al. Three-Dimensional Self-Navigated T2 Mapping for the Detection of Acute Cellular Rejection After Orthotopic Heart Transplantation. Transplant Direct 2017;3(4):e149.
25. Blume U, Lockie T, Stehning C, et al. Interleaved T(1) and T(2) relaxation time mapping for cardiac applications. J Magn Reson Imaging 2009;29(2):480–487.
26. Jones JA, Hodgkinson P, Barker AL, Hore PJ. Optimal sampling strategies for the measurement of spin-spin relaxation times. J Magn Reson B 1996;113(1):25–34.
27. Bustin A, Rashid I, Cruz G, et al. 3D whole-heart isotropic sub-millimeter resolution coronary magnetic resonance angiography with non-rigid motion-compensated PROST. J Cardiovasc Magn Reson 2020;22(1):24.
28. Odille F, Escanyé JM, Atkinson D, Bonnemains L, Felblinger J. Nonrigid registration improves MRI T2 quantification in heart transplant patient follow-up. J Magn Reson Imaging 2015;42(1):168–174.
29. Bönner F, Janzarik N, Jacoby C, et al. Myocardial T2 mapping reveals age- and sex-related differences in volunteers. J Cardiovasc Magn Reson 2015;17(1):9.